Multi-terminal Josephson Junctions

Mesoscopic quantum cavities in proximity to N superconducting leads

A Bachelor Project

Written by

Tobias Born Clausen

Supervised by

Prof. Charles M. Marcus

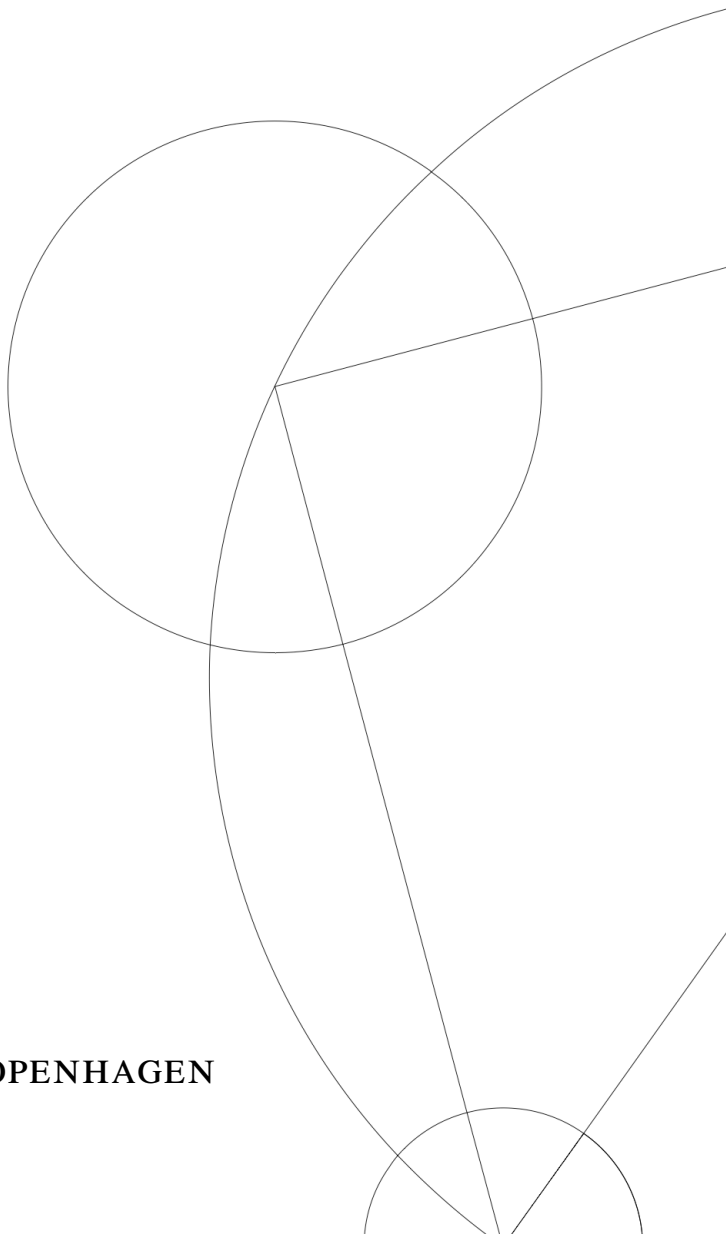

University of Copenhagen

FACULTY:	SCIENCE	
INSTITUTE:	Niels Bohr Institute	
AUTHORS:	Tobias Born Clausen	KU-ID: TWM816
EMAIL:	twm816@alumni.ku.dk	twm816@ku.dk
TITLE:	Multi-terminal Josephson-Junctions	
SUPERVISOR:	Prof. Charles M. Marcus marcus@nbi.ku.dk	
CO-SUPERVISOR:	PhD Cand. Magnus R. Lykkegaard magnus.lykkegaard@nbi.ku.dk	
HANDED IN:	16^{st} of June	

Abstract

In this project, chapter 1 explores some of the physics of multi-terminal Jospehson junctions (MTJJs), by covering preliminary concepts for understanding Jospehson junctions (Chapter 0), the Jospehson effect , Andreev scattering in a multi-terminal setup, and Weyl points driving the MTJJs topologically non-trivial.

I reflect over, in chapter 2, the steps involved when working at a quantum device laboratory, such as material considerations, design the chip and the devices taking into considering aspects of the Josephson effect and Andreev scattering, fabrication steps leading to a measurable device, and measurement techniques supporting and employing different instruments.

Then in chapter 3, how observation of quartet Cooper-pairs, the critical current contour and the number of modes into each terminal are key to measure the controllability of the interface between terminals and junction and reflecting upon the device fabrication process could amount to the desired measurable characteristics of a MTJJs, applying chapter 1 and 2, and basing it on earlier works done in the field.

Abstract

I dette projekt udforsker jeg nogle af de fundamentale fysiske egenskaber for multi-terminal Jospehson kontakter (MTJJs). Jeg dækker grundlæggende viden for at forstå Josephson kontakter, herunder forklarer Josephson effekten, Andreev spredning i et multi-terminal system og Weyl knuder, som

Jeg reflekterer over grundlæggende trin for arbejdet i et kvante-enheds-laboratorie, såsom overvejelser af materiale, at designe en kvante-enhed med henblik på at tage højde for Josephson effekten og Andreev spredning, de endelige fremstillings trin op til at stå med en målbar enhed, og de målings teknikker der bliver taget brug af.

Jeg tag fat i observationen af kvartet Cooper-par, konturen for kritisk strøm og antallet af tilstande i hver terminal afgørende for at måle styrbarheden af grænsefladen mellem terminaler og kontakter. Dette reflekterer også over processen med at fremstille enheden og kan føre til de ønskede målbare karakteristika for MTJJs.

Acknowledgements

Working in the Topological 2DEG group of QDev at University of Copenhagen, has both been an academic challenge and an important insight into the everyday life of an quantum device experimentalist, reflected in following the teachings of my co-supervisor, Magnus Lykkegaard, day-to-day. From the introduction to Magnus by Charles M. Marcus, further to an amazing team at the Quantum Matter group meetings, who all have had me blown away in their own work within the field.

I am thankful of the time and effort Magnus put into his guidance, alongside his own phd, with the clean room laboratory, QCoDeS, and measurement techniques. I owe alot of insight and guidence into the literature to him.

Contents

CHAPTER 0

Introduction

The Josephson effect was predicted theoretically by Brian Josephson in 1962 [1], where in the following year it was confirmed experimentally [2]. Since then the literature has expanded with large numbers of articles and books, exploring and explaining the unique quantum features of this effect, and with tremendous progress in fabrication technology, we see various applications of the Josephson junctions. It was realized that Josephson junctions had potential applications as fast switching devices in digital circuits [3], today they show purposeful in superconducting qubits and circuits within the field of quantum computers and information processing. The research till today has resulted in circuits of many different types of Josephson junctions, of which the multi-terminal Josephson junctions has emerged, with many questions on their nature and performances [4]. As a Bachelor student, I therefore seek forward in this Bachelor project, to showcase my introductory understanding of the physics underlying Josephson junctions, when they are expanded to multiple terminals, and in relation to experimental physics in a quantum device laboratory.

To further understand these Josephson junctions I introduce some preliminary concepts.

0.1 Superconductivity

On the topic of superconductivity, a wide range of superconductive elements and expansive knowledge is now know today, since its discovery in 1911 by Onnes [3]. Of which, a zero resistance state forms in the superconductor, when cooled below a critical temperature [3]. A state vulnerable to disruption by a sufficiently large magnetic field, or by a current exceeding a critical amount [3].

0.1.1 Reaching Critical Depth

In 1933, it was shown that the magnetic fields passing through the material at high temperatures, were evicted as the temperature reached critical, inducing superconductivity [5]. The temperature dependence of the critical magnetic field, illustrated in 1.

This eviction is known as the Meissner effect. For further explanation, consider Ampere's law, there must be a current emerging below the critical temperature, running across the surface of the superconductor, producing a magnetic field exterior to the superconductor, which screens the interior from magnetic fields [3]. The screening current, which is not driven by an electric field, instead just exists by itself, does not decay with time, as a result of the zero resistance state [3].

The eviction of the magnetic fields does not abruptly stop at the surface, the London brothers finds it penetrates a short distance into the surface, called the London penetration depth λ. Further, beyond a depth, but a distance at which the transitioning to a superconductive state occurs from a region with no superconductivity, was proposed by Pippard, as the coherence length ξ_0 [3]. Applying this length for an interface between a superconductor and a non-superconductor, there is then a continuous transition to zero magnetic field, a coherence length into the non-superconductor, illustrated in 1b.

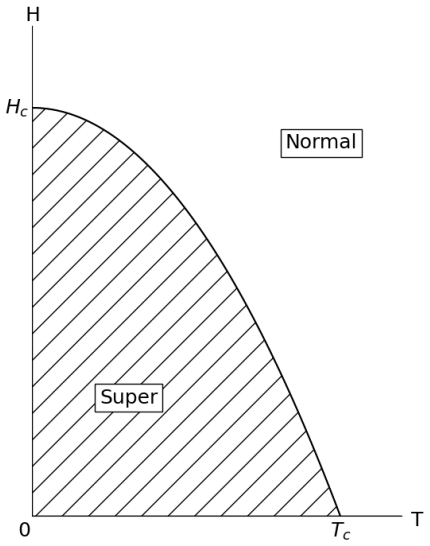

(a) *Temperature dependence of critical magnetic field*

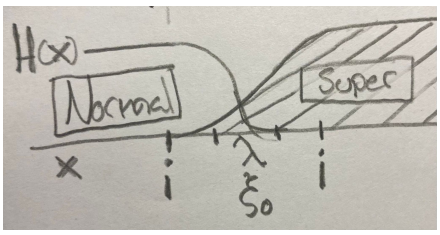

(b) *Penetration depths*

Figure 1: *Figures adapted from Introduction to Superconductivity by Micheal Thinkham [6].*

Going critical

Currents driven by an electric field, passing through the superconductor, induce a magnetic field. The magnetic field, at a critical current $\mathbf{I_c}$, will exceed the critical field at the surface of the superconductor, disrupting the superconducting state [7]. Reversing of the superconducting state into the normal state is attributed to an exterior magnetic field sufficiently large enough to outdo the induced magnetic field from the screening current.

0.1.2 Currents

With the prediction of tunneling currents, in the form of electron pairs, between two superconductors by Jospehson in 1962[1]. The idea of electrons pairing is tackled by looking at the problem of the the many interacting electrons and impose, they be condensed to a Fermi sea [3]. A term proposed by Leon Cooper, that described how only looking at two interacting electrons in a sea of frozen electrons would lead to the stable Cooper pair, rather than single electrons [3]. This interaction had to be a weak attractive interaction, described by John Bardeen and colleague, for the electron pairing to occur [3]. To explain the interaction, in metal, electrons are attracted to positively charged ions in a lattice, the attraction distorts the ions and creates a region, which a second electron will be attracted to, the two electrons pairs up [3]. They over-

come their mutual repulsion, at a spatial length about ξ_0 [3]. The excitations and interactions that arise from the collective behaviour of Cooper pairs are refereed to as quasi-particles. To describe the two electrons in the Cooper pair; their momentum will be equal and opposite with opposite spin, $(\mathbf{k}\uparrow, -\mathbf{k}\downarrow)$, with respect to each other [3]. This results in the Cooper pair having zero spin.

Three great minds

In superconductors the different Cooper pairs would have to be spaced apart and avoid collision, as colliding means disrupting the superconducting state [3]. It is to be understood that Cooper pairs carries superconductivity. I introduce here how the minds of Barden, Cooper and Robert Schrieffer handles this problem. Schrieffer manages to describe the superconducting state as a wave function, $\psi(\mathbf{r})$, not with a fixed number of independent electrons [3]. He varies the number of electrons connected to an electron reservoir, heavily relying on quantum superposition for electrons going in and out of existence [3]. Attributing all individual electrons wave function with a phase, the BCS wave function:

$$\psi(\mathbf{r}) = |\psi(\mathbf{r})| \exp\{i\phi(\mathbf{r})\},$$

all electrons could have the same single phase when superconducting, which in turn tackled collisions (scattering) [3]. The phase coherence holds for macroscopic distances and factors [6]. This meant, all pairs would move together at the same speed, as a deviating pair would be more costly in terms of energy [3]. This uniformly movement of electrons represent a current flowing through the sample, never decaying.

A strength to the BCS wave function interpretation arise when accounting for scattering events, which occurs from impurities or off the different electrons, excluding coherent Cooper pairs. A scattering interacting results in one pair scattering into another pair, such when thinking of the system, as all the individual pairs together, nothing changes [3]. The intermediate state in the scattering process, before forming a new pair, can be regarded as the electrons being in a superposition - jumping out into the electron reservoir.

Mind the gap

The attracting movements of electrons inside a metal, cost essentially nothing, this is not the case for insulators, for which I remind you of energy gaps, which non-intuitively for a superconducting state of Cooper pairs is found to be present [3]. To move an electron, dependent on how tightly it is bound, less or more energy is required, denoted as the energy gap. For a superconducting state, the electron is stuck in an Cooper pair. The explanation of an energy gap, arise as you think of not only exciting an electron but also the energy required to break the Cooper pair [3]. The energy gap acts a buffer, of the size equal to the binding energy of the Cooper pair [3]. This buffer can get preemptively filled by thermal energy, such that the energy gap disappears, electrons halts their pairing, so no energy is needed to break the Cooper

pair [3]. This explains that for superconductivity to occur, a superconductor needs to be cooled below a critical temperature, reflecting the energy gap is temperature dependent. Oppositely, we can think of the Cooper pairs coupling with an energy exceeding the thermal energy k_bT at temperature T [8].

0.1.3 Vortices

Forming Cooper pairs to make the superconducting state, is a saving of energy. Toward the surface, over a coherence length, the superconducting wave function decays to zero [3]. The number of pairs falls, such that not enough energy is saved to account for fully excluding a magnetic field [3]. Not having this abrupt stop costs less energy, allowing the magnetic field to penetrate the London depth. In the bulk of a superconductor the savings outweigh the costs, there is a balance of energy [3].

A superconductor which expresses a longer penetration depth than coherence length, has a screwed energy balance - the energy to allow magnetic fields to penetrate succeeds, destroying superconductivity [3]. Interfaces of normal regions, with magnetic fields penetrating, and superconducting regions are energetically favourable, a Type II superconductor [3]. The regions of magnetic fields, shown by Alexei Abrikosov, forms tubes, containing a quantum of magnetic flux, Φ_0, shielded from the superconducting region by currents flowing around each tube, denoted by the flow as vortices [3]. In literature, knwon as the Schubnikov phase, defined within the boundary of H_{c_1} and H_{c_2}, as illustrated in 2, [6]. Not strangely the vortices exhibits structure, as they arrange themselves into triangular lattice [3]. These vortices react to a supercurrent flowing in the superconductor by a resultant force in a transverse direction, avoiding current dissipation, impurities keep the vortices in place [3].

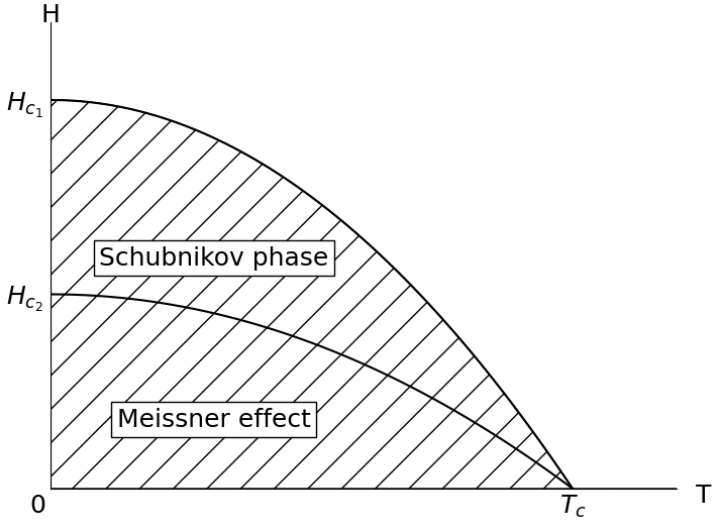

Figure 2: *The Schubnikov phase, figure adapted from Introduction to Superconductivity by Micheal Thinkham [6].*

CHAPTER 1

Multi-terminal Jospehson junctions

In this chapter I strive to further explore currents, here across multi-terminal Josephson junction (MTJJs), by covering two microscopic effects. These are the Andreev reflection and proximity effect. In such I provide an introduction to Andreev bound states, explaining their formation in the cavity of MTJJs. Discussing the unique properties of ABS, such as their energy spectra and their relation to the underlying symmetries of the system.

1.1 The Josephson Effect

A Josephson junction consist of two superconductors separated by a normal region, a cavity. A supercurrent, I_s, flows through the normal region, only slightly changing the Cooper pair density in the two separated superconducting regions, recognized as the Josephson effect [9]. We can interpret this current as the wave functions of each superconductor overlapping in the normal region [4]. This overlap can be reflected by the wave functions extending beyond their coherence length, as discussed in 0.1.1. The wave function carries the flow of Cooper pairs from the superconductor through the normal region, the electrons phase coherence decay after some time, before which the normal region is weakly superconductive [8]. This reflects why it is called the proximity effect, for which it is only the normal region in proximity to the superconductor that inhibits Cooper pairs.

The supercurrent is expressed by an dependence on the phase difference, $\Delta\phi$, of two separated superconducting regions,

$$I_s(\phi) = I_c \sin \Delta\phi \tag{1.1.1}$$

the current-phase relation (CPR) spring forward, though it should be noted it is not always on the form of (1.1.1) [10]. Here think back that I_c is the critical current, the maximum current the junction can support. Which reaches a lower limit, derived from the coupling energy $E_J = \hbar I_c/2e$, at $I_c > 2ek_bT/\hbar$ [8]. An alternative current, AC, Josephson effect, means the phase difference is subjected to a voltage difference, V, across the junction, by $\mathrm{d}(\Delta\phi)/\mathrm{d}t = 2eV/\hbar$ [8]. From this, recognize that the AC current takes on an amplitude of I_c and frequency, $\nu = 2eV/h$. The frequency reflects how often a Cooper pair flows across the junction, from which it follows a change of quantum energy equaling $h\nu$ [8].

1.2 Andreev Scattering

An aspect of the proximity effect is Andreev reflection, AR, which describes what actually goes on more precisely, when we say a current flows from the normal region through to the superconductor. Recognize here that the proximity effect is the time-reversed effect. At this interface an electron undergoes scattering: an electron ($\mathbf{k}\uparrow$) is reflected as a hole ($\mathbf{k}\downarrow$) along the same trajectory as the electron came in with [4]. This creation and the destruction of electrons and holes is viewed as the particle-hole symmetry. The reflection happens due to a single electron being prohibited from moving into the superconductor, there is no space for the quasi-particle with energy $E < \Delta$, as described in 0.1.2. To fulfill a Cooper pair, ($\mathbf{k}\uparrow, -\mathbf{k}\downarrow$), the normal region adds in an extra electron with ($-\mathbf{k}\downarrow$). It then follows to see a Cooper pair in the superconductor, there is a charge difference between the electron and the hole of $2e$ [4].

With the superconducting gap being constrained to the Fermi level, and alignment of the Fermi energy, E_F, between the superconductor and normal region, the superconductor accepts Cooper pairs at the Fermi energy [11]. Excitation a little above the Fermi level for the electron, E, and a little below for the hole, $-E$, and the superconductor phase, ϕ_S, results in a phase shift acquired from AR (proximity effect) by the hole (electron) [12],

$$\phi_{h(e)} = \arccos \frac{E}{\Delta} \mp \phi_S \tag{1.2.1}$$

From their energy $|E| > 0$, a momentum difference between the hole and electron arise, $\Delta k = k_e - k_h$, the hole does not follow the trajectory of the electron, excess momentum Δk is absorbed by the Cooper pair [13].

1.2.1 Josephson junction

We now extend AR to a junction, a S-N-S, where two S-N interfaces arise over a distance of L_J. At both superconductors the gap Δ is the same and their phases differ by Φ. The normal region between them sees a boundary at L_1 and L_2, of which $L_J = L_2 - L_1$. Between the two interfaces an electron (hole), with $|E| < \Delta$, gets AR (Proximity effect) at both interfaces, a cycle. A cycle reflects a supercurrent running across the junction slightly changing the Cooper pair density in the two separated superconductors. The number of AR, multiple AR (MAR) or nth-order AR, meaning flowing across the normal region $n + 1$ times.

A clear separation of states above and below Δ reflects an attribute of hardness to the gap. The quasi-particles are confined, bound states, leading to discrete energy levels [12]. The discrete energy levels, arise by a phase periodicity of the total phase shift, $\phi_{total} = 2\pi n$, during a cycle, derived from 1.2.1 [12]:

$$\phi_{total} = L_j \Delta k + 2 \arccos E/\Delta - \Phi, \tag{1.2.2}$$

The discrete energies, denoted Andreev bound states (ABS), the total number of energy levels, m, are attributed to the number of AR, n, and the two lowest energies, for the limit of the short junction ($L_J << \xi_o$), take on the form [12],

$$E_{ABS} = \pm\Delta \cos \Phi/2 \tag{1.2.3}$$

We recognize here that the two lowest energies exhibit a symmetry around the Fermi energy, one can argue that there is time-reversal symmetry for the two energies. Should the cycle be reversed, then by particle-hole symmetry, the two energies would be related.

These energies are valid when the only scattering are at the interfaces, in the case of impurities in the normal region, scattering occurs, which we account by τ [12]. A fraction, reflecting the ABS transmitting through the impurity, such that [12],

$$E_{ABS} = \pm\Delta\sqrt{1 - \tau \sin^2 \Phi/2} \tag{1.2.4}$$

It then follows that the supercurrent, Cooper pairs, flow, from the normal region through to the superconductor, is mediated by the ABS, denoted at finite temperature as [12],

$$I_{s_{ABS}} = \frac{2e}{\hbar} \sum_{n=0}^{m} \frac{\mathrm{d}E_n}{\mathrm{d}\Phi} \tanh \frac{E_n}{2k_b T} \tag{1.2.5}$$

Where $n = 1, 2, 3, ..., m$ takes into account the number of discrete energy states that are available for ABS, up to a total of m. The multiple number of discrete energy state exhibits level spacing, a consequence of time-reversal symmetry and particle-hole symmetry. The supercurrent sees a dependency on the transmission, τ, such that at $\tau = 1$ there is full transmission through the impurities, meaning the highest supercurrent [12].

1.2.2 Weyl points

When the right conditions befall the ABS energy spectrum, the lowest energy band can sink down to zero at a specific phase, called a Weyl point [14]. Remembering back to the discussed time-reversal for the electron and hole, a Weyl point reflects two states collapsing to zero energy. The Weyl point act as a topological defect, modifying the Cooper pair, resulting in no absorbed momentum difference, as discussed above. A isolated Weyl point can thereby be topologically protected [14]. This feature of being topologically protected, translate to the MTJJs as being topologically non-trivial [14].

To locate the Weyl point at a specific phase, Φ, which reflects the difference between multiple superconductor phases, each phase can be adjusted to result in Φ. For n superconductors, one of the phases can be left at $\phi_0 = 0$ without affecting the others [14]. This means there are $n - 1$ independent phases to turn, reflecting a $(n - 1)$D phase space wherein Weyl points appear [14].

CHAPTER 2

Materials And Methods

This chapter is meant to reflect the steps, from deciding on the chip to having a device loaded for measurements, including enabling measurability.

The device of interest in this project is an InGaAs/InAs 2DEG epitaxial Al heterostructure grown and provided by the Manfra group at Purdue University. Grown bottom-up by a Molecular Beam Epitaxy system (MBE) on the substrate InP.

From top to bottom of the heterostructure, a layer of Al on top, grown *in situ*, refereed above to as epitaxial, reflecting the Al were grown along with the heterostructure in the MBE without breaking vacuum, acquiring an unspoiled interface with the heterostructure [15]. Below a layer confines electrons along the growth direction of the device to a ”narrow” quantum well (QW), allowing the electrons to only move perpendicular to the growth direction, forming a 2DEG [15]. The QW is reflected in the layer of InGaAs-InAs-InGaAs in the heterostructure structure. Here two larger band gap materials, InGaAs, enclose a smaller band gap material, InAs, forming the QW [12]. The Al layer sits in close proximity to the QW, the proximity effect is not negligible [12], superconductive properties arise in the QW, as discussed in chapter 1. Opposite of the Al layer sits a layer of InAlAs, constricting the QW in the downward direction, by having a larger band gap than InGaAs [11]. The last layers of InAlAs in the heterostructure acts as a buffer, buffering the transition from the InP substrate to the QW layers to ensuring a good interface [12].

2.1 Design

Designing chips means creating a Computer Assited Drawing (CAD) file, capable being converted into formats for Design computers to interpret and make readable for fabrication machines. Designing should reflect a number of devices, the size of the chip make it doable to do multiple design variations of devices and duplicates - safety for anomalies in fabrication.

The arrangement of multiple superconducting leads should be reflected when designing the devices, a geometry of leads should allow for MAR within the cavity of MTJJs. The leads should be controllable in the sense, the design will allow for connecting inner parts, cavity, of the device to bonding parts by gates. Controllable, reflecting it is doable to make a number of leads

non-desirable for AR - non-superconducting leads. The design should account for placement of alignment marks and bonding pads, reflecting that bonding will not overlap between devices.

To induce the short junction in a device, as discussed in 1.2.1, the design should take into account making the junction length, L_j, much shorter than the decoherence length. Short enough to ensure a measurable supercurrent would flow between two neighbouring superconductors, discussed in 1.1. This is were anomalies in fabrication can arise, reflecting the design was too optimistic, too short a length between junction. With foresight, designing different variations, from which devices can be inspected under a scanning electron microscope (SEM) and chosen from, can result in optimal junction length.

2.2 Fabrication

As a start point, chips of the grown wafers are cleaved into a suitable size. The cleaved chip is inspected under a SEM, to look for undesirable surface regions. The SEM is used to inspect and document each step, when allowed for. With a chip, and a prepared design file, which reflects the complete device, etching of mesa and alignment marks will start as the first major fabrication steps.

The chips are cleaned to allow to start with one of many spin resists, PMMA4 A4. Spin resist refers to the spin coating of the chip, such that while spinning the chip at high speeds, a liquid spin resist is deposited on top of the device.

A mesa etch outlines a rough template of the device, to only etch out the desired part of the chip, a mask, resistant to etching, is laid out. This mask is a coating of spin resist laid out evenly across the chip. Regions of the spin resist, defined by the design, is exposed to an electron beam, by an electron beam lithography (E-Beam), leaving it more soluble. The next step is then to remove the soluble spin resist - develop. Leaving spin resist, not hit by electrons, protecting, soon to be, platforms for bonding pads and ohmic contacts. As next step is etching the heterostructure, removing layers down to the substrate, constricting current to platforms. The need for spin resist on top of the platforms is gone, so return the state of the chip to being without any resist - stripping remaining resist off.

The alignment marks, etched as crosses, serves as reference points when precisely aligning the different steps of the device fabrication. These marks, by design, sits on the outer regions of the chip.

For Al etch, the chip undergoes the E-Beam and development process, resist PMMA A2, and using the alignment marks, an Al pattern from the design is etched into the chip. It is understood that, from the epitaxial Al layer, everything except the Al patterned in the design is etched away.

After stripping the remaining resist, the chip is transferred directly to the atomic layer deposition (ALD). Not allowing for imaging in SEM. The ALD deposition a single atomic layer of the

material, Hf, on top of the chip. Further, the layer forms into an oxide of HfO_2 from water vapour. This cycle is repeated 150 times to form a desired height onto the chip. The desired height is based on HfO_2 electrically insulating properties. The layer insulate previous layers from the next layer of Au_2/Ti_2 gates.

Repeating the E-Beam and development process, with PMMA A4.5, ALD is followed by metal evaporation (AJA) of the materials making up the gates, Au_2 and Ti_2.The Au_2/Ti_2 is evaporated by the heat of an electron beam. A desired rate is reached by adjusting the beam, after which a shutter is opened, allowing for deposition. The deposition happen in order of Ti_2 first, because Au_2 sit more firmly on Ti_2 than HfO_2. The Au_2 evaporation follows after a slow cooling period. The layer of Au_2/Ti_2 is patterned to the design by removing developed resist underneath the layer, a lift off. The actual gates where done in two steps, separating into inner gates and outer gates, where outer connects inner to bonding pads. The two stages then separates from each other by the settings of the E-beam, defining precision, details uncovered after a lift off.

2.3 Measurement technique

Doing the fabrication of the device, measures where taken to allow for electrical contact with the device the bonding pads. The bonding pads acts as highways for external instruments to measure the device by running along ohmic contacts and gates. Connected by a thin wire to a daughter-board, which allows for a limited communicating - number of DC lines and channels that can be connected to a motherboard. The limitations of channels allows for only some devices on the chip, chosen by previous imaging, to be measured. The motherboard is a experimentalist way to get communicating with devices, taking the highways - establishing a connection to the outside of a cryostat. A cryostat houses a puck, whitin sits the motherboard, connecting wires running up through the cyostat and out into a breakout box to the experimentalist's measurement instruments.

2.3.1 Lock-in Amplifiers

A measurement instrument of interest, translates how the device responds to electrical signals, a low frequency Lock-in Amplifier (LIA). It is the job of a LIA to measure noise of signals close to a reference frequency, at which the signal can be amplified while minimizing the impact of noise [16]. A desired frequency is chosen for the electrical signals exciting the device, making it possible to eliminate noise from measurements [16]. Before the signal reaches back to a LIA, it is either current amplified through a BASEL I/V converter or voltage amplified by a ETH. From this signal, noise is eliminated outside of the detection bandwidth, which is dependent on the the low-pass-filter time constant [16]. One of a few settings to get the signal just right. Another one of these settings is the dynamic reserve, an aspect of the LIA in its digital variant, it reflects the tolerated noise to signal ratio [16].

2.3.2 QCoDeS

For data acquisition from measurement instruments, the laboratory takes use of the software QCoDeS, a python-based framework [17]. QCoDeS allows for setting up a connection to the instruments, allowing readoffs directly to the software [17]. Of particular use was the do1d/do2d multi-dimensional measurement utility. The do1d creates an experiment: do1d(running a independent parameter, through an interval, with a number of steps, waiting at each step by an amount, followed by dependent parameters (LIA and Digital multimeter)). The data is stored in a database and can be easily plotted for one, by adding in the keyword "$do\_plot = True$" [17].

2.3.3 Reaching Critical Temperature

The power to cool materials below the discussed temperature dependency of superconductivity, in Chapter 0, is essential for measurements. A further dependence arise from ABS. Cooling to such temperatures, the power of a cryofree dilution refrigeration is required, the Triton cryofree dilution refrigeration, which cools down to an observed 14mK, is just right for that job. This refrigerator has the puck loaded from the bottom, allowing for a easier switch out and in of chips. The 14mK refers to the temperature of the mixing chamber of which the device is connected through the puck. Mentioning of the mixing chamber refers to the inside of the refrigerator, alongside which, a still exist [18]. These two components give an simple idea of how cooling of the device happens. A look at the phenomena of cooling-by-mixing: sees that from the mixing of a diluted $He^3 - He^4$ phase and a concentrated phase of He^3, follows an positive enthalpy change [18]. The mixing requires energy from surroundings, cooling the mixing chamber. The still comes into the picture by aiding in circulating helium, keeping the process of cooling-by-mixing alive by [18]. Further, the aspect of the refrigerator being cryofree, reflects a precooling of He^3 via pulse tube cooling, mediated by heat exchangers [18]. A weekly task in the laboratory was refilling a carbon filter with liquid nitrogen, a filter connected up to the pulse tube cooler.

CHAPTER 3

Observations

I acknowledged here in conclusion, instead of measurement results, how it would look observing quartet Cooper-pairs, the critical current contour (CCC) and the number of modes into each terminal, as they are key to measure the controllability of the interface between terminals and junctions.

3.1 Critical Current Contour

The maximal current, I_c, a short junction can support in the device, as discussed in 1.2.1, can be observed in a I-V curve by a experiment made with QCoDeS. By applying a bias, a supercurrent, and a resulting phase difference (Voltage), discussed in 1.1, a contour then relates their relationship to the critical current, as the transition in the contour to zero voltage (superconducting state) the maximal current the junction can support is expressed. Here it should be observed that the transitioning to superconductive state from normal state, expresses different critical current [11].

Reflecting theoretically the number of modes, N, as the ABS carrying the supercurrent, discussed in 1.2.1, observed in the short junction, should be related to the critical current by $I_c = N\frac{e\Delta}{\hbar}$ [19]. The observation should be taking impurities in the junction into account, to a point of being able to recognize, a the transmission dependence of the supercurrent, discussed in 1.2.1.

3.2 Quartet Cooper-pairs

It should be observed from MTJJs and MAR, as discussed in 1.2.1, that biasing multiple leads, and our design allowing the cavity being proximitized, should result in quasiparticles forming two entangled Cooper pairs - quartet Cooper pair [20]. The observation of a quartet Cooper pair should be clear in a 2D plot for differential conductance, $G_j = \delta I_j/\delta V$, from an excitation signal δV and current δI_j (LIA), as a function of the DC bias voltage V_j and a predetermined V_k, [20].

CHAPTER 4

Bibliography

[1] B. D. Josephson. Possible new effects in superconductive tunnelling. Physics letters, 1 (7):251–253, 1962.

[2] P. W. Anderson and J. M. Rowell. Probable observation of the josephson superconducting tunneling effect. Physical Review Letters, 10(6):230, 1963.

[3] S. J. Blundell. Superconductivity: A Very Short Introduction. Oxford University Press, 05 2009. ISBN 9780199540907. doi: 10.1093/actrade/9780199540907.001.0001. URL https://doi.org/10.1093/actrade/9780199540907.001.0001.

[4] F. Tafuri. Fundamentals and Frontiers of the Josephson Effect, chapter 1, Introductory Notes on the Josephson Effect: Main Concepts and Phenomenology, pages 1–61. Springer International Publishing, Cham, 01 2019. ISBN 978-3-030-20724-3. doi: 10.1007/978-3-030-20726-7. URL https://doi.org/10.1007/978-3-030-20726-7_1.

[5] W. Meissner and R. Ochsenfel. A new effect concerning the onset of superconductivity. Die Naturwissenschaften, 21:787, 1933.

[6] M. Tinkham. Introduction to superconductivity, chapter 1, Introductory Survey. Scientific International, 2017.

[7] N. W. Ashcroft and N. D. Mermin. Solid State Physics. Harcourt College Publishers, 1976.

[8] M. Tinkham. Introduction to superconductivity, 2017.

[9] R. Kleiner and H. Wang. Fundamentals and Frontiers of the Josephson Effect, chapter 10, Intrinsic Josephson Junctions in High Temperature Superconductors, pages 367–439. Springer International Publishing, Cham, 01 2019. ISBN 978-3-030-20724-3. doi: 10.1007/978-3-030-20726-7. URL https://doi.org/10.1007/978-3-030-20726-7_1.

[10] A. A. Golubov S. V. Bakurskiy and M. Yu. Kupriyanov. Fundamentals and Frontiers of the Josephson Effect, chapter 3, Basic Properties of the Josephson Effect, pages 81–105. Springer International Publishing, Cham, 01 2019. ISBN 978-3-030-20724-3. doi: 10.1007/978-3-030-20726-7. URL https://doi.org/10.1007/978-3-030-20726-7_1.

[11] M. Kjaergaard. Proximity Induced Superconducting Properties In One And Two

Dimensional Semiconductors, chapter II, superconducting properties of the epitaxial al/i-nas quantum well. 2015.

[12] A. M. Whiticar. Quantum Transport: Introduction to Nanoscience, page 22–33. Cambridge University Press, 2020.

[13] Y. V. Nazarov and Y. M. Blanter . Scattering, page 7–123. Cambridge University Press, 2009. doi: 10.1017/CBO9780511626906.003.

[14] RP. Riwar, M. Houzet, and et al. J. Meyer. Multi-terminal josephson junctions as topological matter. Nature Communications, 7, 2016.

[15] M. Kjaergaard. Proximity Induced Superconducting Properties In One And Two Dimensional Semiconductors, chapter I basic concepts fabrication. 2015.

[16] About lock-in amplifiers. Stanford Research Systems, Application Note 3. URL `https://www.thinksrs.com/downloads/pdfs/applicationnotes/AboutLIAs.pdf`.

[17] Microsoft Corporation and Københavns Universitet. Qcodes, 2015-2023. Accessed June 15, 2023. `https://qcodes.github.io/Qcodes/index.html`.

[18] F. Pobell. Matter and Methods at Low Temperatures, chapter 7, The 3He–4He Dilution Refrigerator, pages 149–176. Springer Berlin, Heidelberg, 01 2007. ISBN 978-3-540-46360-3. doi: https://doi.org/10.1007/978-3-540-46360-3.

[19] C. W. J. Beenakker. Three "universal" mesoscopic josephson effects. In Springer Series in Solid-State Sciences, pages 235–253. Springer Berlin Heidelberg, 1992. doi: 10.1007/978-3-642-84818-6_22. URL `https://doi.org/10.1007%2F978-3-642-84818-6_22`.

[20] K. Huang and et al. Y. Ronen. Evidence for 4e charge of cooper quartets in a biased multi-terminal graphene-based josephson junction. Nature Communications, 13(3032), 2022. doi: https://doi.org/10.1038/s41467-022-30732-7.